EXPERIMENTAL NEUROLOGY 128, 41–49 (1994)

Mammalian Cortical Astrocytes Align Themselves in a Physiological Voltage Gradient

RICHARD B. BORGENS, RIYI SHI, THOMAS J. MOHR, AND CHRISTINE B. JAEGER

Center for Paralysis Research, School of Veterinary Medicine, Purdue University, West Lafayette, Indiana 47907-1244

Astrocytes obtained from primary cultures of newborn rat cerebral cortex show a marked structural rearrangement to weak (50–500 mV/mm) applied voltage gradients. Astrocytes reorient their processes so that the cells are aligned perpendicular to the voltage gradient. At field strengths of 100 mV/mm or greater, this realignment occurs in over 90% of the cell population. Furthermore, these magnitudes of electric fields completely eliminate any parallel alignments originally observed prior to application of the voltage. Realignment usually occurs by a withdrawal, followed by an extension, of cell processes. These responses occur at voltage gradients within the physiological range that naturally exist across the neural tube during early development. We suggest the possibility that architectural arrangements of developing glia and, subsequently, neurons may be regulated by endogenous transepithelial potentials that exist across embryonic neuroepithelium.

INTRODUCTION

It is generally not appreciated that cells developing within the vertebrate embryo reside in a polarized gradient of voltage. Steady ionic current is driven out of the lateral walls of the neural folds in both *Xenopus laevis* and *Ambystoma mexicanum* neurulae and out of the blastopore (29). These steady currents traverse the amphibian embryo during the entire period of neurulation, the neural fold currents disappearing at fusion of the neural folds. The associated gradients of voltage beneath the neural plate are about 10–20 mV/mm and are caudally negative with respect to rostral regions of the embryo. Following closure of the neural folds a substantial potential (ca. 15 mV) is expressed across the walls of the anuran neural tube (17). This transneuroepithelial potential would result in an electrical field of about 500 mV/mm across the 30-μm-wide neural tube, and exceeds 1 V/mm in urodele embryos (38).

Artificially applied, weak, steady voltages are also known to affect development and regeneration of the nervous system (3, 4). Applied fields (25–75 mV/mm) imposed across developing neurulae in an attempt to scramble the symmetry of the endogenous voltage gradients produce gross distortions of development, suggesting the endogenous fields provide important cues for developing embryonic pattern (28). Applied extracellular voltages can also produce a facilitated regeneration of identified CNS axons in severed lamprey spinal cord and intracellularly marked dorsal column axons in the adult guinea pig spinal cord (7, 9). In the latter, evidence of CNS regeneration is associated with functional recovery of a long tract reflex [the cutaneus trunci muscle (CTM) reflex] when the applied electric field is imposed at the time of injury, but not when delayed by 3 months (5, 6, 8, 10).

In all, a primary cellular target of the applied voltage is presumed to be the neuron. Growing neurites and regenerating axons are well known to be responsive to weak applied voltages that can orientate their growth—usually toward the cathode—as well as increase the rate of elongation and branching of regenerating axons (3, 4). Cells of glial lineage also play an important role during the growth and regeneration of the nervous system. During development glial processes provide a scaffolding for the subsequent migration of developing neurons (33), while ependymal cells may play a similar role facilitating regeneration of spinal cord axons in fish, amphibians, and reptiles (1, 39, 40). It is entirely unknown, however, if the migration or the structural alignment of glial cells can be directed by a weak extracellular voltage. Using cultured rat cortical astrocytes [immunocytochemically positive for glial fibrillary acidic protein (GFAP)], we show that extracellular voltages in the range of 50–500 mV/mm can profoundly organize the populations of these cells perpendicular to the applied voltage gradient.

METHODS AND MATERIALS

Cell Cultures

The population of cells investigated was obtained from satellite cultures of dissociated cortex from newborn rats. Cells were grown for 2 weeks, subcultured, and cryo-preserved until use. Glia cells were isolated from dissociated cerebral cortex of newborn rats accord-

0014-4886/94 $6.00

ing to procedures described by McCarthy and DeVellis (26). The primary cells were grown in 20-ml culture flasks for 10–14 days. The growth medium consisted of basal Eagle's medium with Hank's salt (Gibco), containing 30 m*M* glucose, 15% fetal bovine serum, and 50 units/ml penicillin/streptomycin. Subcultures were prepared from flasks that had grown to confluency. At this stage, rounded cells, which overlie the flat polygonal astrocytes, were removed by brief treatment (30 s) with Ca^{2+}, Mg^{2+}-free phosphate-buffered salt solution containing 0.05% trypsin. Loosely adhering cells floated off into the supernatent which was discarded and enzyme activity was inhibited by addition of growth medium. Adhering cells were mechanically dislodged from the flask surface by forceful aspiration of the medium with a Pasteur pipette. Suspensions of dissociated cells (approximately 1×10^5/ml) were plated onto poly-L-lysine-coated glass ($2 \times 25 \times 0.1$ mm) and allowed to adhere to this substrate. After various times of preincubation (16–72 h) the coverslips were placed into the chambers for observation and field exposure. At the termination of the experiment, cultures were fixed for 10 min in 4% paraformaldehyde dissolved in 0.1 *M* phosphate buffer (pH 7.4). Cultures were incubated overnight with one of either polyclonal GFAP antisera (ARKO) diluted 1:2000 or monoclonal GFAP antisera (Boehringer) diluted 1:100 in Tris-buffered saline containing 1% serum. Staining of astroglia was carried out with indirect immunocytochemistry utilizing a peroxidase anti-peroxidase procedure previously described by Jaeger (20).

Application of Electrical Fields

Preliminary experiments using both focally applied and uniform electrical fields demonstrated that: (a) astrocytes respond to both focally applied (nonuniform) and uniform extracellular voltage gradients. Response to the latter, however, is more dramatic and repeatable; (b) GFAP-positive astrocytes would orientate themselves in uniform gradients of voltage on the order of 100–300 mV/mm (Fig. 1); and (c) that 78% of the cell population comprising these test cultures was GFAP positive (Fig. 1). These preliminary observations led to improvements in the design of a special chamber (Fig. 2) which would allow visualization and photography of large numbers of cultured cells at two to four locations by conventional microscopy as well as simultaneous recording of cell behavior by high-resolution, VHS, time-lapse video microscopy.

This chamber was placed on the stage of a Nikon Diaphot inverted microscope fitted with a Plexiglas incubation chamber held to 37 ± 0.3°C with a thermostatically controlled heater. Coverslips with adherent cells were placed into a slot within the test chamber and a thin layer of mineral oil was applied to the surface of the culture medium to control both evaporation and pH change due to gas exchange at the medium's surface. Temperature was monitored continuously during the experiment using an indwelling microthermoprobe. Fields were applied using a regulated power supply, and the voltage drop produced across the cells was both calculated (Ohm's law) and directly measured (refer to Fig. 2). A standard VHS recording paradigm was usually used, where 10 s of record was taken every 4 min. Video images were retrieved by frame grab and image analysis software on a MAC IICi computer using Rastor Ops, Media Grabber 1.7, and I.P. Lab Spectrum. The angles of orientation were scribed onto the image using Image 1.47 software.

Analysis of Cell Orientation

The population responses to imposed uniform fields (50–500 mV/mm) were evaluated by producing an overlay for each 8 × 10 photographic field of view (two or three fields of view/culture), on which was scribed each cell perimeter and scored to depict its long axis of symmetry. Initially, cells were defined as perpendicular if this long axis was within 15° normal to the long axis of the voltage gradient, parallel if within 15° of parallel, tangential if the cell's axis fell outside these criterion, and isodiametric if no axis of symmetry could be determined. These scoring procedures were performed by a person blinded to the experimental status of the cultures. Using this method, orientational changes in cell populations were first evaluated at field strengths of 230 and 320 mV/mm.

These initial data suggested that the character of the population's response could be achieved by analyzing those cells possessing a definable axis of symmetry at the beginning of the experiment. To evaluate this, an index of cell asymmetry (AI) was calculated for all cells in all subsequent experiments [asymmetry index (AI) = $(n > 45°) - (n < 45°)/(n < 45°) + (n > 45°)$ (16)]. This index produces values from −1 to 1; −1 indicates that every cell in the field of view was aligned parallel to the long axis of the applied field and +1 indicates that every cell in the field of view is aligned perpendicular to the long axis of the applied field. Three-dimensional graphs plotting field strength × asymmetry index × time in culture were constructed using Stastica software where a surface plot is obtained by a least squares analysis. Data points at the intersects are represented in two

FIG. 1. (a) GFAP immunocytochemistry of primary cultures 2 weeks after initial isolation (15). Random counts of 400 cells were made to obtain a measure of GFAP-positive astroglia within the cultures. In 10 separate cultures an average of 78% of the cells was GFAP positive. (b) Phase-contrast photomicrographs of astrocytes growing in the experimental chamber prior to field exposure. (c) Fifteen hours after current flow from top to bottom (voltage gradient = 320 mV/mm), the cells exhibit a striking perpendicular alignment.

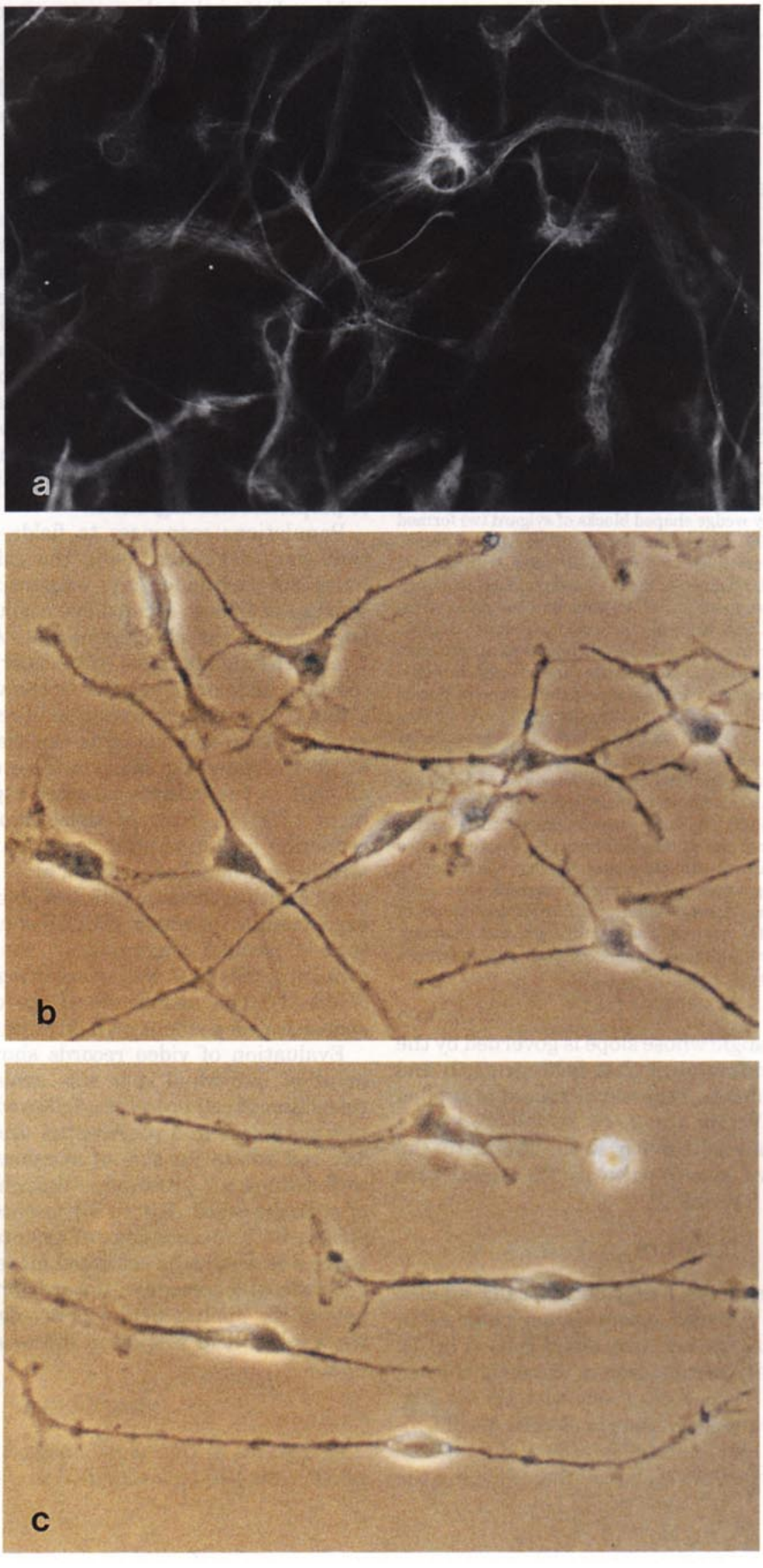
a
b
c

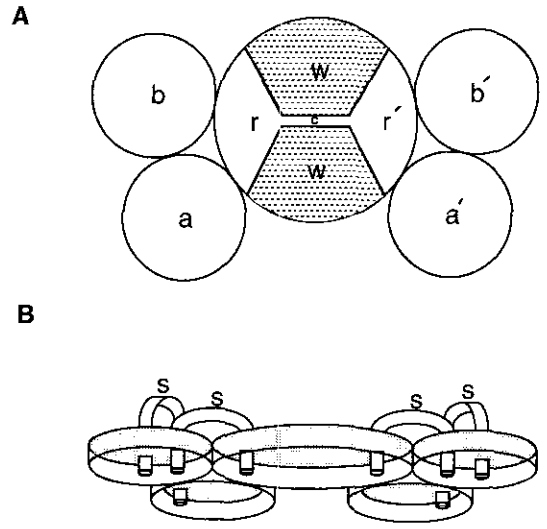

FIG. 2. Cells attached to coverslips were placed in a specially designed chamber (A) for electric field imposition containing slot c. This slot (c) was formed by wedge shaped blocks of sylgard (w) formed within the Petri dish (100 mm) using a mold. Reservoirs r and r' continuous with slot c were filled to a depth of 2 mm with culture medium. Four 60-mm petri dishes (a, b, a', b') were affixed as shown and also filled with culture medium. When the chamber cover (B) is placed over the chamber, salt bridges (s) formed of 4-mm i.d. glass tubing filled with 2% agar in culture media (without serum) provided electrical connection. Coiled AgAgCl electrodes (anode and cathode) were placed in chambers a and a'. In this arrangement current flowed in series through a, b, r, slot c (containing the cells), r', b', and a'. This completely separates cells in slot c from electrode products produced at the electrode/medium interface at a and a'. The electric field was calculated using Ohm's Law by multiplying the measured resistivity of the medium (86 Ωcm) with the current density traversing the slot (c). This was derived by dividing the total current passed through the circuit by the cross-sectional area of the slot (0.04 cm^2). This estimated potential drop was confirmed directly using AgAgCl electrodes to measure the potential drop across slot (c) while the current was turned "on" and "off." This voltage was not monitored during the conduct of the experiment. The total current passed through the chamber, however, was monitored continuously during each experiment using a multimeter inserted in series.

dimensions as a rectangle whose slope is governed by the asymmetry index (ordinate) at that field strength and time. In these experiments, cells were exposed to applied fields of 50–500 mV/mm for 7–16 h, followed by a variable period of analysis (1.5–9 h) in the absence of the field. In addition, two control cultures ("0" field) were analyzed for over 21 h (Table 1).

RESULTS

Preliminary experiments using both focally applied and uniform fields revealed orientational changes in GFAP-positive astrocytes and unstained cells (Fig. 1). Immunocytochemical identification of astroglia showed that 78% of the cells stained positively with GFAP (Fig. 1a). The other unstained nonneuronal cells would include immature glia and endothelial cells. Cells exposed to uniform voltage gradients realigned themselves in the field such that their long axis was perpendicular to the applied voltage gradient, compared to control cultures in which cells oriented randomly (Figs. 1b and 1c).

Population responses to the applied fields were first quantitatively evaluated at 230 and 320 mV/mm. Six such experiments were performed, two at 230 mV/mm (mean number of cells per field of view = 56) and four experiments at 320 mV/mm (mean number of cells per field of view = 51). The pooled results of these experiments are presented in Fig. 3. At both field strengths the percentage of the cell population that was perpendicular to the voltage gradient increased markedly within 6–8 h of field exposure. The number of cells originally parallel to the longitudinal axis of the imposed field always decreased (230 mV/mm) and was completely eliminated at 320 mV/mm (Fig. 3B). Eventual reductions in the percentage of the population of isodiametric cells (320 mV/mm) or cells possessing a tangential axis of symmetry (230 and 320 mV/mm) was due to their recruitment to perpendicular alignment.

Populations responses to fields of 50–500 mV/mm that were evaluated using the calculated asymmetry index both extended and emphasized the marked responses of cells to applied extracellular voltages. At the beginning of the experiments, the AI was slightly positive (perpendicular bias) in 10 experiments and negative (parallel bias) in 14 relative to the voltage gradient (see Table I). A striking orientation of cells was evident after exposure to exogenous fields, especially at field strengths of 100 mV/mm or greater. In these experiments, almost all cells in the culture assumed a perpendicular alignment (Fig. 4). Nine of these experiments showed a reduction in the AI after cessation of the field demonstrating a gradual return to a more random orientation of cells within the population (Table 1, Fig. 4). Of the 14 experiments in which the AI showed an initial bias toward parallel alignment at the beginning of field exposure, this bias was overcome in every experiment (Table 1). The magnitude of the cell population's response was dependent on field strength (Fig. 5).

Evaluation of video records showed that the alignment of individual cells was achieved largely by the retraction of cell processes, followed by the extension of new processes in a preferential orientation. Rarely did any cell rotate its axis of symmetry while possessing well-defined cell processes—though we do have records of such an event. Figure 6 presents a cell that demonstrates both mechanisms of orientational change. The somata of some cells exhibited movement, but a general galvantrophic response toward, or away from, either pole of the applied field was not detected. Cessation of the applied field was often followed by process retraction.

DISCUSSION

Astrocytes in this study showed a profound orientational response to an applied extracellular gradient of

TABLE 1

Experiments, Applied Fields, and Asymmetry Index

Culture	Field strength (mV/mm)	Time in (h)[a]	Time out (h)[b]	Mean cells/experiment	AI		
					E_{on}	E_{off}	End
12	0 (controls)	0	21	45	0.2[c]	0.16[d]	0.1
12	0 (controls)	0	21	32	0.1[c]	0.1[d]	0.1
1	50	15.5	5.5	44	−0.12	0.3	0.1
1	50	15.5	5.5	49	−0.24	0.39	0.3
3	100	11	2	29	−0.27	0.39	0.4
3	100	11	2	21	−0.47	0.5	0.25
2	100	15	9	28	−0.7	0.78	0
2	100	15	9	31	0	0.33	0.2
4	100	16	2	61	−0.22	0.43	0.43
4	100	16	2	48	−0.1	0.4	0.43
6	250	8	1.5	29	−0.23	0.64	0.85
6	250	8	1.5	30	−0.09	0.28	0.3
5	250	10	2	60	−0.3	0.45	0.7
5	250	10	2	52	−0.4	0.48	0.4
7	250	11	3	41	0.25	0.56	0.26
7	250	11	3	34	0.25	0.54	0.54
7	250	11	3	25	0	0.88	0.6
8	320	7.5	5.5	73	0.09	0.7	0.52
9	320	7	5	48	0.23	0.62	0.4
9	320	7	5	48	−0.31	0.9	0.54
9	320	7	5	56	0.04	0.83	0.48
10	500	7.5	3	32	−0.11	0.54	0.25
10	500	7.5	3	35	0.03	0.89	0
11	500	10	3	54	0.3	0.88	0.85
11	500	10	3	51	−0.36	0.94	0.68
11	500	10	3	37	0.18	0.85	0.78

[a] Total elapsed time within the electric field (E_{on}).
[b] Total elapsed time following cessation of the field (E_{off}).
[c] AI at the beginning of the 21-h period of observation.
[d] AI at the end of 12 h of observation.

voltage (50–500 mV/mm). They withdrew cell extensions and extruded new ones to align themselves perpendicular to the voltage gradient. Similar responses have been observed in a large number of other nonneuronal cell types including fish epidermal cells (keratocytes) (12), amphibian neural crest (11, 42), embryonic fibroblasts (14, 31), myoblasts (24), and osteoblasts (15) to name a few (see reviews by Robinson 1985; Nuccitelli, 1988; and Borgens, 1992). This common trend toward a perpendicular orientation has been hypothesized to provide the cell a means to expose less cross-sectional area to the voltage across its extremes and thus lessen the amount of depolarization/hyperpolarization of its resting potential caused by the imposed extracellular potential (11). Sometimes the shift to a perpendicular orientation is followed by a marked cell migration toward the cathode (or negative pole) of the applied field. This occurs, for example, in fibroblasts, keratocytes, osteoblasts, and neural crest. This is not always the case, however. Osteoclasts (15) migrate toward the anode, while early myocytes (16) and chondrocytes (Borgens, unpublished observations) orient perpendicular to the field but do not preferentially migrate (in a way similar to the astrocytes described here).

The elongating tip of neuronal processes and myoblast processes also shows a strong migratory response to applied DC fields. The growing tip homes on the cathode and thus the processes themselves show a striking orientation toward the negative pole when cultured on physiological substrates (3, 16, 21, 32). Growth rates are severely retarded in cell processes facing the positive pole (anode) of the applied field or the processes are resorbed completely (16, 19, 21). The strong guidance cue provided by an extracellular voltage gradient can dominate other guidance cues (such as "contact guidance") when both are tested simultaneously (22). The mechanism of action underlying the behavior of cell processes (23) is believed to be related to the specific changes in the gating of Ca^{2+} at the growing tip (3, 4, 23) produced by the field, and a respecification of the position of integral membrane components (IMCs) floating in the plasma membrane by lateral membrane electrophoresis and/or electrosmosis (3, 18, 25). The latter notion is supported by the fact that heavy labeling

of IMCs with Concanavalin A eliminates cell process orientation within applied voltage gradients in both neurons (32) and myoblasts (24). The resorption of a cell process facing the positive pole is less well understood; however, it is clear that the enhanced retrograde degeneration of injured axons facing the anode is caused by increased levels of cytosolic calcium within the severed tip of the fiber produced by the applied voltage (4, 9, 37, 41). Furthermore, severed fibers facing the opposite pole (the cathode) of the applied DC field take up less Ca^{2+} from the extracellular milieu, and also degenerate less, than control fibers (37, 41).

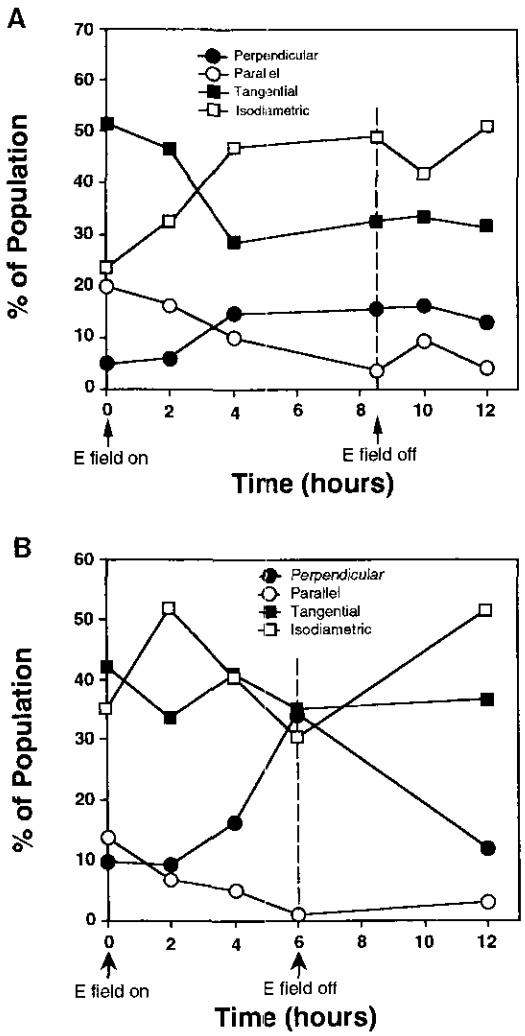

FIG. 3. (A) Orientational changes in cells at 250 mV/mm. The axis of cells scored perpendicular (●), parallel (○), and tangential (■) to the axis of the voltage gradient, as well as isodiametric cells (□), is plotted against time in the applied field and following cessation of the applied field. Note the increase in the population of cells perpendicular to the voltage gradient, and the reduction of parallel oriented cells after 6 h of field exposure. (B) Orientational changes in cells exposed to 320 mV/mm. The general character of the response is the same as depicted in A, only more marked. Note the elimination of parallel oriented cells following field exposure.

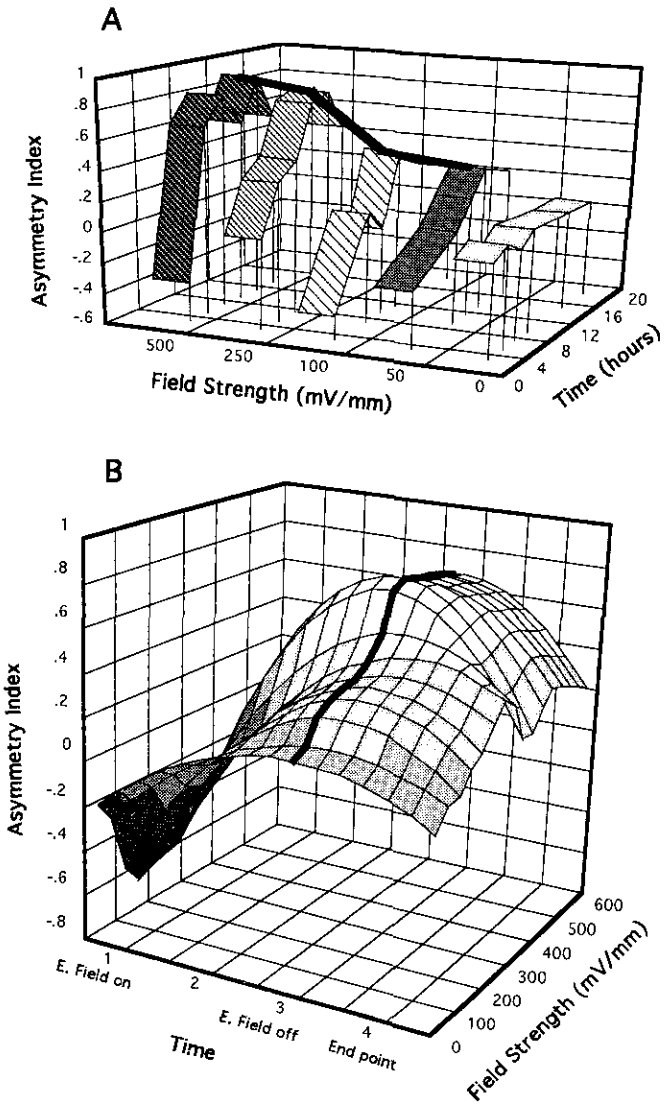

FIG. 4. (A) The AI plotted against time and field strength for four representative experiments (50, 100, 250, and 500 mV/mm) and one of two control experiments. Note the marked increase in perpendicular alignment at the higher magnitude of applied voltage. The bold line connecting each plot denotes the point at which the applied field was removed. (B) AI plotted against field strength and time. The AI for all experiments at all field strengths is plotted against four time points. The data are normalized around the point of field cessation (bold line as above) and the graph fits the data from the lowest AI calculated (dark gray) to the most perpendicular alignment (white). The values for parallel alignment (negative AI) were not extended to −1 as no values fell below those shown. Note the increase in perpendicular alignment at all field strengths tested, and the fall in AI (trend toward random orientation) following the elimination of the applied field.

These cellular responses are important because steady endogenous voltage gradients of the magnitudes tested in this and other studies exist in and around skin wounds (2, 43), regenerating tissues (4, 27), and the embryonic nervous system (28, 29). Glial cells are known to provide a template for neuronal migration and oriented growth during development and regeneration

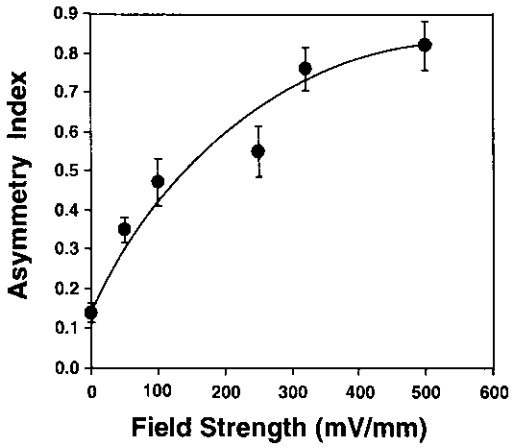

FIG. 5. The average AI and its standard error of the mean (SEM) is shown for all field strengths at the point in time when the field was turned off. The control culture's average AI was taken after 12 h. The coefficient of correlation for these data is 0.94.

(33); however, their responses to physiological voltages have not been described until now.

It is also clear that steady polarized extracellular electric fields (10 mV/mm–1 V/mm) exist during development of the nervous system. Hotary and Robinson (17) report a 15-mV potential across the 30-μm-wide neural tube of stage 22 *Xenopus* embryos. This would result in a field of about 500 mV/mm expressed across these developing cells. In axolotl embryos we have measured much larger transneural tube potentials that increase in magnitude with development to about 85 mV by stage 28 (38). The neural tube is approximately 50 μm wide at this stage of development, resulting in an extracellular voltage gradient expressed across neuroepithelial cells of about 1.7 V/mm.

Recent studies on the orientation of cultured rat hippocampal neurons suggest their processes may respond differently to extracellular voltages, depending on their stage of differentiation and whether the particular process is an axon or dendrite (13, 34). These data and ours suggests a novel manner in which an early "prepat-

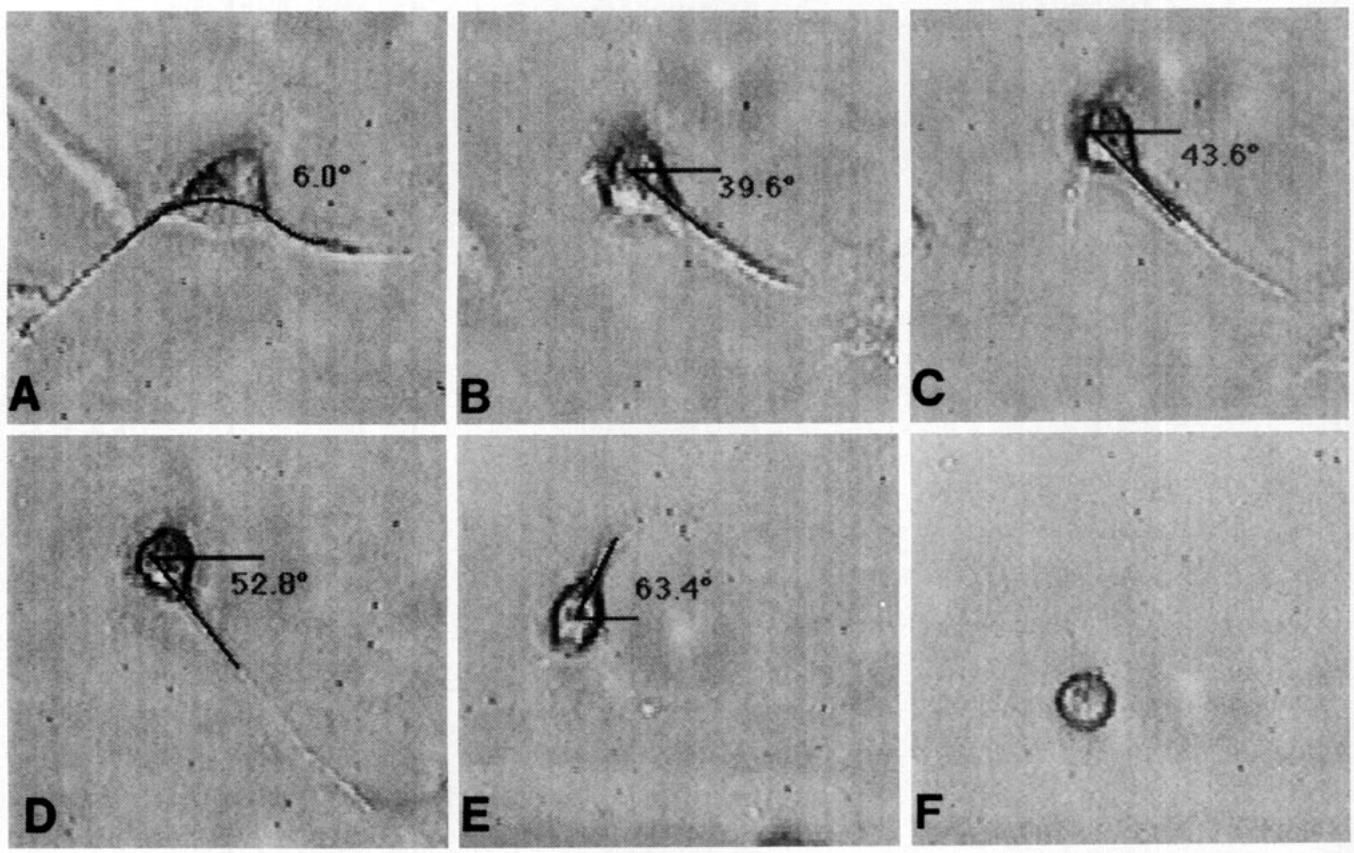

FIG. 6. Videographic analysis of orientational change in a cell and its processes. (A) This bipolar cell had resided in an applied field (200 mV/mm) unchanged for about 150 min. Curve fitting for the index line reveals the axis of this cell to be approximately 6° from parallel with the voltage gradient. (This frame was taken at 116 min from the start of the field application). (B) The cell process facing the anode was retracted leaving the axis of symmetry approximately 40° from parallel after 158 min of field exposure. Clockwise rotation of the cell angle to about 53° from parallel alignment by 304 min of field exposure (D). Within the next 3 h this process was retracted and a new process was extended approximately 63° from parallel (E). The field was turned off and within 15 min the cell retracted this process becoming isodiametric (F). Rotation of the cell body and (cathode facing) process from 24 to 53° was not accompanied by any expanded lamellapodia visible at this magnification.

tern" of cellular architecture may be imposed on differentiating glia and neurons residing within a substantial endogenous gradient of polarized extracellular voltage.

In studies of the field-induced recovery of function of the CTM reflex in spinal cord injured adult guinea pigs, it was determined that delay of the applied voltage following spinal lesioning resulted in a failure in functional recovery (10). Applications of extracellular electric fields by indwelling stimulators applied at the time of spinal cord lesioning resulted in a recovery of the reflex in up to 25% of the experimental animals, but in none of the sham-treated population (5, 6). It is well known that reactive gliosis occurs following CNS injury leading to a sometimes dense and widespread glial cicatrix (35). This so-called "glial scar" has long been implicated as either a physical or physiological barrier to the projections of injured CNS axons. Moreover this putative barrier has been associated with the failure in functional recovery following CNS injury in mammals (35). We note that in our studies where the CTM reflex recovered, this glial cicatrix is forming in the presence of the applied voltage. The glial cicatrix has already formed in experiments where the application of the electric field is delayed (which is associated with a failure in functional recovery). It is not unreasonable to hypothesize that the applied field could affect the orientation of glial cells forming the scar, and that this may be associated with the beneficial effects of applied electric fields following spinal cord injury in adult mammals (5, 6, 8).

ACKNOWLEDGMENTS

We acknowledge the expert technical assistance of Aaron Harbath and Debra Bohnert. We thank Heather Eddy for manuscript preparation. This work was funded by USARMDC Grant DAMD17-91-Z-1008 and support of the Center for Paralysis Research by the Canadian Spinal Research Organization.

REFERENCES

1. ANDERSON, M. J., S. G. WAXMAN, AND M. LAUFER. 1983. Fine structure of regenerated ependyma and spinal cord in *Stenarchus alfifrons*. *Anat. Rec.* **205:** 73–83.
2. BARKER, A. T., L. F. JAFFE, AND J. W. VANABLE, JR. 1982. The glabrous epidermis of cavies contains a powerful battery. *Am. J. Physiol.* **242:** R358–366.
3. BORGENS, R. B., AND C. D. MCCAIG. 1989. Artificially controlling axonal regeneration and development by applied electric fields. In *Electric Fields in Vertebrate Repair* (R. B. Borgens, K. R. Robinson, J. W. Vanable, Jr., and M. E. McGinnis, Eds.), Chap. 4, pp. 117–170. Liss, New York.
4. BORGENS, R. B. 1992. Applied voltages in spinal cord reconstruction: History, strategies, and behavioural models. In *Spinal Cord Dysfunction,* Vol. III, *Functional Stimulation,* pp. 110–145. Oxford Univ. Press, Oxford.
5. BORGENS, R. B., A. R. BLIGHT, AND M. E. MCGINNIS. 1987. Behavioral recovery induced by applied electric fields after spinal cord hemisection in guinea pig. *Science* **238:** 366–369.
6. BORGENS, R. B., A. R. BLIGHT, AND M. E. MCGINNIS. 1990. Functional recovery after spinal cord hemisection in guinea pigs: The effects of applied electric fields. *J. Comp. Neurol.* **296:** 634–653.
7. BORGENS, R. B., A. R. BLIGHT, D. J. MURPHY, AND L. STEWART. 1986. Transected dorsal column axons within the guinea pig spinal cord regenerate in the presence of an applied electric field. *J. Comp. Neurol.* **250:** 168–180.
8. BORGENS, R. B., J. P. TOOMBS, A. R. BLIGHT, M. S. BAUER, W. R. WIDMER, AND J. R. COOK. 1993. Effects of applied electric fields on clinical cases of complete paraplegia in dogs. *Restor. Neurol. Neurosci.* **5:** 305–322.
9. BORGENS, R. B., L. F. JAFFE, AND M. J. COHEN. 1980. Large and persistent electrical currents enter the transected spinal cord of the lamprey eel. *Proc. Natl. Acad. Sci. USA* **77:** 1209–1213.
10. BORGENS, R. B., M. E. METCALF, AND A. R. BLIGHT. 1993. Delayed application of Direct Current Electric Fields in Experimental Spinal Cord Injuries. *Restor. Neurol. Neurosci.* **5:** 173–179.
11. COOPER, M. S., AND R. E. KELLER. 1984. Perpendicular orientation and directional migration of amphibian neural crest cells in DC electrical fields. *Proc. Natl. Acad. Sci. USA* **81:** 160–164.
12. COOPER, M. S., AND M. SCHLIWA. 1984. Motility of cultured fish epidermal cells in the presence and absence of direct current electric fields. *J. Cell Biol.* **102:** 1384–1399.
13. DAVENPORT R. W., AND C. D. MCCAIG. 1993. Hippocampal growth cone responses to focally applied electric fields. *J. Neurobiol.* **24:** 89–100.
14. ERICKSON, C. A., AND R. NUCCITELLI. 1984. Embryonic fibroblast motility and orientation can be influenced by physiological electric fields. *J. Cell Biol.* **98:** 296–307.
15. FERRIER, J., S. M. ROSS, J. KANEHISA, AND J. E. AUBIN. 1986. Osteoclasts and osteoblasts migrate in opposite directions in response to a constant electric field. *J. Cell Physiol.* **129:** 283–288.
16. HINKLE, L., C. D. MCCAIG, AND K. R. ROBINSON. 1981. The direction of growth of differentiating neurons and myoblasts from frog embryos in an applied electric field, *J. Physiol.* **314:** 121–135.
17. HOTARY, K. B., AND ROBINSON, K. R. 1991. The neural tube of the *Xenopus* embryo maintains a potential difference across itself. *Dev. Brain Res.* **59:** 65–73.
18. JAFFE, L. F. 1977. Electrophoresis along cell membranes. *Nature* **265:** 600–602.
19. JAFFE, L. F., AND M.-M. POO. 1979. Neurites grow faster toward the cathode than the anode in a steady field. *J. Exp. Zool.* **209:** 115–127.
20. JAEGER, C. B. 1988. Plasticity of astroglia: Evidence supporting process elongation by "stretch." *Glia* **1:** 31–38.
21. MCCAIG, C. D. 1986. Dynamic aspects of amphibian neurite growth and the effects of an applied electric field. *J. Physiol.* **375:** 55–69.
22. MCCAIG, C. D. 1986. Electric fields, contact guidance and the direction of nerve growth. *J. Embryol. Exp. Morph.* **94:** 245–255.
23. MCCAIG, C. D. 1989. On the mechanism of nerve galvanotropism. *Biol. Bull.* **176:** 136–139.
24. MCCAIG, C. D., AND P. J. DOVER. 1989. On the mechanism of oriented myoblast differentiation in an applied electric field. *Biol. Bull.* **176S:** 140–144.
25. MCLAUGHLIN, S., AND M-M. POO. 1981. The role of electro-osmosis in the electric field induced movement of charged macromolecules on the surfaces of cells. *Biophys. J.* **34:** 85–93.
26. MCCARTHY, K. D., AND J. DEVILLIS. 1980. Preparation of separate astroglia and oligodendroglial cell cultures from rat cerebral tissue. *J. Cell. Biol.* **85:** 890–902.
27. MCGINNIS, M. E., AND J. W. VANABLE, JR. 1986. Electrical fields in

Notophthalmus viridescens limb stumps. *Dev. Biol.* **116:** 184–193.

28. METCALF, M. E., AND R. B. BORGENS. 1994. Weak applied voltages interfere with amphibian morphogenesis and pattern *J. Expt. Zool.* **268:** 322–338.
29. METCALF, M. E., R. SHI, AND R. B. BORGENS. 1994. Endogenous ionic currents and voltages in amphibian embryos. *J. Expt. Zool.* **268:** 307–322.
30. NUCCITELLI, R. 1988. Physiological electric fields can influence cell motility, growth, and polarity. *Adv. Cell Biol.* **2:** 213–233.
31. NUCCITELLI, R., AND C. A. ERICKSON. 1983. Embryonic cell motility can be guided by physiological electrical fields. *Exp. Cell Res.* **147:** 195–201.
32. PATEL, N., AND M-M. POO. 1982. Orientation of neurite growth by extracellular electric fields. *J. Neurosci.* **2:** 483–496.
33. PURVES, D., AND J. W. LICHTMAN. 1990. Neuronal migration. In *Principles of Neural Development,* pp. 90–104. Sinauer Associates, Sunderland, MA.
34. RAJNICEK, A. M., N. A. R. GOW, AND C. D. MCCAIG. 1992. Electric field induced orientation of rat hippocampal neurones in vitro. *Exp. Physiol.* **77:** 229–232.
35. REIER, P. J., L. J. STENSAAS, AND L. GUTH. 1983. The astrocytic scar as an impediment to regeneration in the central nervous system. In *Neuroelectric Research* (C. C. Kao, R. P. Bunge, and R. J. Reier, Eds.), pp. 163–195. Thomas, Springfield, IL.
36. ROBINSON, K. R. 1985. The responses of cells to electrical fields, a review. *J. Cell Biol.* **101:** 2023–2027.
37. ROEDERER, E., N. H. GOLDBERG, AND M. J. COHEN. 1983. Modification of retrograde degeneration in transected spinal axons of the lamprey by applied DC current. *J. Neurosci.* **3:** 153–160.
38. SHI, R., AND R. B. BORGENS 1994. Embryonic neuroepithelium sodium transport, the resulting physiological potential, and cranial development. *Dev. Biol.,* in press.
39. SIMPSON, S. B. 1983. Fasciculation and guidance of regenerating central axons by the ependyma. In *Neuroelectric Research* (C. C. Kao, R. P. Bunge, and R. J. Reier, Eds.), pp. 151–161. Thomas, Springfield, IL.
40. STENSAAS, L. J. 1983. Regeneration in the spinal cord of the newt, *Notopthalmus (triturus) pyrrhogaster.* In *Spinal Cord Regeneration* (R. P. Bunge and P. J. Reier, Eds.), pp. 121–149. Raven Press, New York.
41. STRAUTMAN, A. F., R. J. COOK, AND K. R. ROBINSON. 1990. The distribution of free calcium in transected spinal axons and its modulation by applied electrical fields. *J. Neurosci.* **10:** 3564–3575.
42. STUMP, R. T., AND K. R. ROBINSON. 1983. *Xenopus* neural crest cell migration in an applied electrical field. *J. Cell Biol.* **97:** 1226–1233.
43. VANABLE, J. W., JR. 1989. Integumentary potentials and wound healing. In *Electric Fields in Vertebrate Repair* (R. B. Borgens, K. R. Robinson, J. W. Vanable, Jr., and M. E. McGinnis, Eds.), Chap. 5, pp. 171–224. Liss, New York.